CERN-INTC-2000-024

CERN/INTC 2000-024
INTC/P128
April 26, 2000
Beam Time Request to the INTC

Beta-decay study of neutron-rich Tl, Pb, and Bi by means of the pulsed-release technique and resonant laser ionisation

S. Franchoo[1,2], A. Andreyev[2], J. Äystö[1,3], D.V. Fedorov[4], V.N. Fedoseyev[5], H. Fynbo[1], M. Górska[2], H. Grawe[6], R. Grzywacz[7,8], G. Huber[9], M. Huyse[2], Z. Janas[6,8], A. Jokinen[3], M. Karny[7,8], U. Köster[1], V. Kurcewicz[8], J. Lettry[1], V.I. Mishin[5], T. Nilsson[1], M. Oinonen[1], M. Pfützner[8], A. Płochocki[8], K. Rykaczewski[8,10], H.L. Ravn[1], M.D. Seliverstov[4], H. Simon[1], J. Szerypo[3], W. Urban[8], P. Van Duppen[2], L. Weissman[1], and J. Żylicz[8]

[1] CERN ISOLDE, CH-1211 Genève 23, Switzerland
[2] University of Leuven, B-3001 Leuven, Belgium
[3] University of Jyväskylä, FIN-40351 Jyväskylä, Finland
[4] Petersburg Nuclear Physics Institute, RU-188350 Gatchina, Russia
[5] Institute of Spectroscopy, RU-142190 Troitsk, Russia
[6] GSI, D-64291 Darmstadt, Germany
[7] University of Tennessee, Knoxville TN-37996, USA
[8] University of Warsaw, PL-00681 Warszawa, Poland
[9] University of Mainz, D-55099 Mainz, Germany
[10] ORNL, Oak Ridge TN-37830, USA

Spokesperson: S. Franchoo
Contact person: S. Franchoo

Abstract: It is proposed to study new neutron-rich nuclei around the $Z = 82$ magic shell closure, with major relevance for understanding the evolution of nuclear structure at extreme isospin values. Following the IS354 experiment, β-decay studies of neutron-rich thallium, lead and bismuth isotopes will be performed for $215 \leq A \leq 219$. To this purpose the pulsed-release technique, which was pioneered at ISOLDE, will be optimised. It will be complemented with the higher element selectivity that can be obtained by the unique features of resonant laser ionisation, available at ISOLDE from the RILIS source.

1. Introduction

The neutron-rich Tl, Pb and Bi isotopes are of exceptional interest to trace the evolution of nuclear structure and single-particle levels away from the doubly magic ^{208}Pb towards the neutron-rich side of the nuclear chart. While plenty of literature is available on ^{208}Pb, a nucleus which is well understood in terms of the shell model, experimental data on lead isotopes beyond $A = 214$ is very scarce. Shell-model calculations with the Kuo-Hertling interaction have been performed up to $A = 212$ by Warburton and Brown [War91]. Considerable effort has been put in Relativistic Mean Field theory, mainly with respect

a. Mass chain 215

A β-gated γ spectrum recorded at mass 215 for a collection time of 12 seconds only is reproduced in Fig. 2. This short measurement led to the discovery of a new high-spin structure, which probably is to be ascribed to ^{215}Bi^{m} [Plo00]. The single-particle configuration of the isomer has not been established unequivocally and it is not understood why the apparent β decay of this state would be competitive with the IT deexcitation mode. Hence it is not excluded that the observed γ transitions from high-lying states in the ^{215}Po daughter nucleus do not arise from the β decay of ^{215}Bi^{m} but rather from the γ decay of an unknown ^{215}Po^{m} isomer.

No convincing evidence was found to attribute any of the detected γ rays to a new isotope ^{215}Pb, which nevertheless should have been produced in a sufficient amount. Neither an anomaly in the cross-section behaviour nor explanations related to the nuclear structure are satisfactory. However, the analysis of the collected data was complicated by the presence of an intense ^{205}At contamination, which was deposited during a preceding run. Therefore, a renewed investigation focused on ^{215}Pb and relying on resonant laser ionisation is necessary to formulate a definite answer regarding the identity of the observed activity.

b. Mass chain 216

The β decay of ^{216}Bi has been detected and a weak indication for the decay of a new isotope ^{216}Pb found [Ryk98,Kur00]. A half-life of 135(5) s has been measured for ^{216}Bi, whereas previous measurements reported contradictory half-lives of 7(2) m [Bur89] and 3.6(4) m [Ruc90]. The discrepancy might be due to contaminations in the earlier samples. Based on the observation of β feeding to the 8^+ level of the broken $\pi h^2_{9/2}$ pair in ^{216}Po, a high-spin configuration is inferred for ^{216}Bi, likely resulting from the $\pi h_{9/2} \otimes \nu g_{9/2}$ coupling. A possible low-spin state, known in the odd-odd bismuth isotopes at lower mass, has not been seen but could not be excluded either.

c. Mass chain 217

The β decay of the newly discovered isotope ^{217}Bi has been disclosed and the first half-life determination of ^{217}Po performed [Ryk98]. The half-life fits yield 93(3) s for the β decay of ^{217}Bi and 1.53(3) s for the α decay of ^{217}Po. The β decay of ^{213}Pb, which is the daughter product of ^{217}Po, has equally been studied and the level scheme of ^{213}Bi extended. Also for this mass chain, contamination by francium and its daughter nuclides was assessed but hampering the analysis only in a minor way.

3. Beta decay of Tl, Pb, and Bi

In the present proposal we intend to combine the pulsed release with the element selectivity of the RILIS laser ion source. The latter is indispensable, as only the comparison of the spectra recorded with and without laser irradiation will ultimately allow for the unequivocal identification of the γ rays originating from the species of interest. Indeed, despite their short half-lives, the francium, and to some extent also the radium and actinium isotopes, may still contaminate the samples collected by pulsed release. First of all, these isotopes are produced in enormous quantities in the spallation of a UC_2 or ThC_2 target by a 1.4-GeV proton beam (Fig. 3). Secondly, because of their low work functions, they may be extracted from the source through surface ionisation.

Recently laser ionisation schemes have been developed for Tl, Pb, and Bi, yielding efficiencies of respectively 27, 6, and 6%. Since in addition we plan to analyse in detail the release profiles from the ion source in order to improve the pulsed-release technique, this approach will allow to extend the β-decay studies to heavier lead, bismuth, and thallium isotopes.

Since the pulsed-release technique relies on the relatively long lifetimes of the β-decaying isotopes of interest compared to the significantly shorter lived Fr, Ra, and Ac α emitters, the method enables to investigate the mass chains 215 up to 219. According to the FRDM [Moe97], the thallium half-lives stay sufficiently long up to ^{218}Tl, beyond which they could drop below 1 s. The ETFSI model [Bor97] still predicts 20 s for ^{219}Tl (Table 1). For the lead and bismuth isotopes up to $A = 220$, the FRDM projects half-lives longer than 1 s. The experiment would proceed with the study of laser-ionised ^{215}Pb. At this mass we aim to characterise unambiguously the previously observed high-spin structure. The decay of ^{216}Pb will give access to low-spin states in ^{216}Bi, yielding information on the coupling of the $h_{9/2}$ proton to the $g_{9/2}$ neutrons. For ^{217}Pb we expect to extract the single-particle neutron states in ^{217}Bi. Extension of the systematical investigation to $^{218-219}$Pb would further complete the picture of nuclear structure along $Z = 82$.

The FRDM puts forward a surprisingly huge P_n-value of 99% for ^{215}Tl (Table 1). The measurement of this property will constitute a direct test for the FRDM in this mass region. Note that the only other isotope nearby for which β-delayed neutron emission has been reported is ^{210}Tl with $P_n = 0.007^{+7}_{-4}$ [Ste62]. Half-life measurements, in particular for ^{217}Tl and ^{219}Tl, will shed further light on the discrepancy between the FRDM and ETFSI predictions (Table 1). Another most interesting issue gained from the β decay of $^{215-219}$Tl will be the information on the single-particle structures in $^{215-219}$Pb, where especially the position of the $g_{9/2}$ and $i_{11/2}$ neutron orbitals draws interest.

The occurrence of many high-spin single-particle orbitals in the nuclei to be explored will give rise to several isomeric states. Their magnetic moments can be measured by exploiting the sensitivity of the laser ionisation efficiency to the laser frequencies, a method proven to be successfull for probing hyperfine splittings [Koe00]. To this respect, a separate letter of intent is being prepared that aims at a systematic study of g-factors and isotope shifts in the neutron-rich Tl, Pb, and Bi isotopes [Hub00].

4. Experimental setup

A new compact detection chamber will be constructed in order to maximise the solid angle covered by the surrounding detectors. The β-γ coincidence set-up will comprise a number of high-efficiency Ge γ detectors from the Miniball array, a LeGe X-ray detector, and a cooled Si(Li) electron detector. The cooled Si(Li) detector will help to spot conversion electrons superimposed on the β spectrum, while moreover it will enable to remove

contaminant α-delayed events from the data. Additional β scintillators in front of the Ge detectors will further increase the β-γ coincidence efficiency.
Replacement of the cooled Si(Li) detector by the dedicated ELLI conversion-electron spectrometer [Par91] during part of the allocated beam time is envisaged. The separate installation of a neutron detector is foreseen whenever γ rays belonging to adjacent mass chains are observed, aiming at the determination of neutron branching ratios. At the same time, all of the proposed technical developments are meant to contribute to the installation of a permanent detection station for nuclear spectroscopy experiments at ISOLDE. Finally, we point out that the possibility to measure conversion electrons of heavy bismuth isotopes in Rextrap is being investigated independently [Wei00].

5. Beam time request

The production yields for lead and bismuth isotopes have been determined during a test run for experiment IS354 with the plasma ion source and are printed in Fig. 4. From a logarithmic extrapolation of these values we expect about 100 ions/μC for ^{219}Bi and 10 ions/μC for ^{219}Pb. Although the quoted figures were obtained for a 1.0 GeV proton beam on a 55 g/cm^2 ThC_2 target, the energy increase of the proton beam to 1.4 GeV or an eventual change to a UC_2 target should not influence the rates in a major way [Sch00].
From Fig. 3, it would follow that the cross sections for thallium are one order of magnitude lower than those for lead. If we assess the ionisation efficiency of the then used plasma ion source at 30%, we deduce the production rates in the target for the Tl, Pb, and Bi of interest presented in Table 2. Taking into account the laser ionisation efficiencies mentioned before and an estimated β-γ coincidence efficiency of 3%, we put forward the measurement times and projected number of counts, likewise listed in Table 2. Judging from the theoretical half-lives that are compiled in Table 1, decay losses are expected not to be significant. An inspection of Table 2 now demonstrates the feasibility of the experiment.
The figures of Table 2 have been calculated for an average of 3 proton pulses per supercycle and a primary beam intensity of 3×10^{13} protons per pulse. The time structure of the proton beam, however, should depend on the half-life of the isotope to be investigated. For half-lives in the range of 2 to 5 seconds, it is preferable to have all three pulses in the beginning of the supercycle. Shorter half-lives are better accommodated with three equidistant pulses, while longer half-lives require one supercycle with several proton pulses followed by two or three supercycles without sample collection.
To investigate the 5 mass chains ranging from 215 to 219, a number of 12 shifts is thus requested. In order to identify the resonant signal, the same number without laser irradiation is asked for. We foresee 6 additional shifts for conversion electron spectroscopy with ELLI and 6 for a search of neutron emission from the thallium isotopes. Tuning the lasers should take up 1 shift for every element. The total requested beam time therefore equals 39 shifts.

References

[Bor97] I. Borzov et al., Nucl. Phys. A621, 307c (1997)
[Bur89] D.G. Burke et al., ZPA 333, 131 (1989)
[Dob94] J. Dobaczewski et al., PRL 72, 981 (1994)
[Hub00] G. Huber et al., Letter of Intent to the INTC, to be submitted
[Koe00] U. Köster et al., NIM B 160, 528 (2000)
[Kra93] K.-L. Kratz et al, APJ 403, 216 (1993)
[Kur00] J. Kurpeta et al., EPJ A7, 49 (2000)
[Moe97] P. Möller, J.R. Nix, and K.-L. Kratz, ADNDT 66, 131 (1997)
[Par91] J. Parmonen et al., NIM A 306, 504 (1991)
[Plo00] A. Płochocki et al., to be published
[Pfu98] M. Pfuetzner et al., Phys. Lett. B 444, 32 (1998)
[Rau98] T. Rauscher et al., Phys. Rev. C 57, 2031 (1998)
[Rei95] P.-G. Reinhard and H. Flocard, NPA 584, 467 (1995)
[Rei00] P.-G. Reinhard, private communication
[Ruc90] E. Ruchowska et al., JPG 16, 255 (1990)
[Ryk96] K. Rykaczewski et al., Proposal to the Isolde Committee, CERN/ISC 96-1 (1996)
[Ryk98] K. Rykaczewski et al., Proc. Int. Conf. on Exotic Nuclei and Atomic Masses, Bellaire, 1998, AIP 1998, p. 581
[Sch00] K.H. Schmidt, Nucl. Phys. A542, 699 (1992) and private communication
[Ste62] G. Stetter, Nucl. Sci. Abstr. 16, 1409 (1962)
[Van98] P. Van Duppen et al., Nucl. Instr. Meth. B 134, 267 (1998)
[War91] E.K. Warburton and B.A. Brown, Phys. Rev. C 43, 602 (1991)
[Wei00] L. Weissman, private communication

	Tl			Pb		Bi	
A	$t_{1/2}^{FRDM}$	$t_{1/2}^{ETFSI}$	P_n^{FRDM}	$t_{1/2}^{FRDM}$	P_n^{FRDM}	$t_{1/2}^{FRDM}$	P_n^{FRDM}
214	> 100	–	49	> 100	0	> 100	0
215	20		99	> 100	0	> 100	0
216	7.4		94	> 100	0	> 100	0
217	1.8	24	100	> 100	0	> 100	0
218	2.1	1.2	69	> 100	0	4.1	0
219	0.83	20	100	1.2	0	83	0
220	0.43	0.76	99	8.3	0	7.7	0

Table 1. Theoretical half-lives and neutron branching ratios from the FRDM [Moe97] and ETFSI models [Bor97] for neutron-rich Tl, Pb and Bi

	rate in target/s	ε_{laser}	$\varepsilon_{\beta\gamma}$	Δt	expected number of cts
^{215}Bi	430000	6%	3%	1 h	3 10^6
^{216}Bi	67000	6%	3%	1 h	4 10^5
^{217}Bi	11000	6%	3%	1 h	7 10^4
^{218}Bi	2000	6%	3%	1 h	1 10^4
^{219}Bi	330	6%	3%	4 h	9 10^3
^{215}Pb	43000	6%	3%	1 h	3 10^5
^{216}Pb	6700	6%	3%	1 h	4 10^4
^{217}Pb	1100	6%	3%	2 h	1 10^4
^{218}Pb	200	6%	3%	8 h	1 10^4
^{219}Pb	33	6%	3%	24 h	5 10^3
^{215}Tl	4300	27%	3%	1 h	1 10^5
^{216}Tl	670	27%	3%	1 h	2 10^4
^{217}Tl	110	27%	3%	4 h	1 10^4
^{218}Tl	20	27%	3%	16 h	9 10^3
^{219}Tl	3.3	27%	3%	24 h	2 10^3

Table 2. Expected production rates, laser ionisation and β-γ detection efficiencies, projected measurement times and number of counts, calculated for an average of 3 proton pulses per supercycle

Fig. 1. Neutron single particle energies for ^{214}Pb in the HF+SkO' model as a function of the effective mass m^* [Rei00]

Fig. 2. Beta-gated γ spectrum collected for 12 seconds at mass 215 [Ryk98]

Fig. 3. Abrasion-ablation calculations for neutron-rich Tl, Pb, Fr, Ra, and Ac isotopes by 1.4-GeV protons on ^{232}Th [Sch00]

Fig. 4. Production yields for $^{214-217}$Bi and ^{214}Pb measured with the plasma ion source at ISOLDE for 1.0-GeV protons on a 55 g/cm^2 ^{232}ThC$_2$ target. The dashed lines are extrapolations

Fig. 1

Neutron single-particle energies for ^{214}Pb
(HF+SkO')

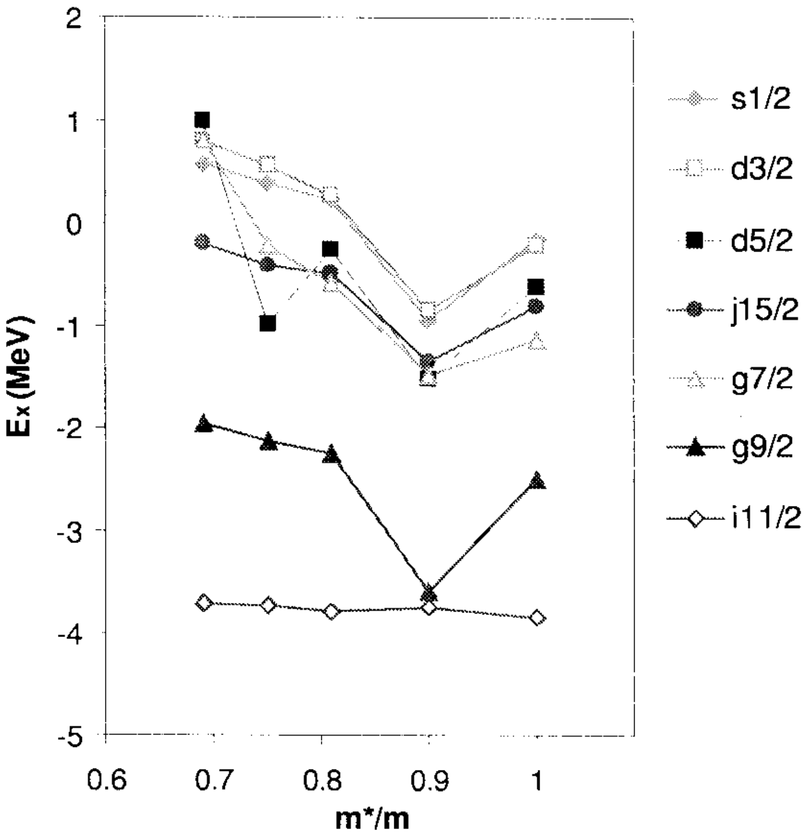

P-G Reinhard, private communication

Fig. 2

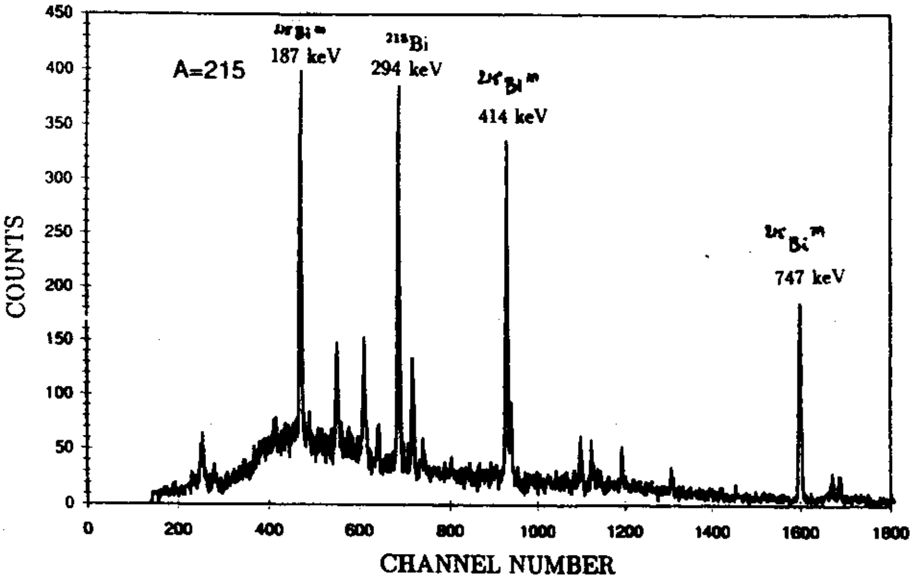
A=215
^{215}Bi^{m}
187 keV
^{215}Bi
294 keV
^{215}Bi^{m}
414 keV
^{215}Bi^{m}
747 keV
COUNTS
450
400
350
300
250
200
150
100
50
0
0
200
400
600
800
1000
1200
1400
1600
1800
CHANNEL NUMBER

Fig. 3

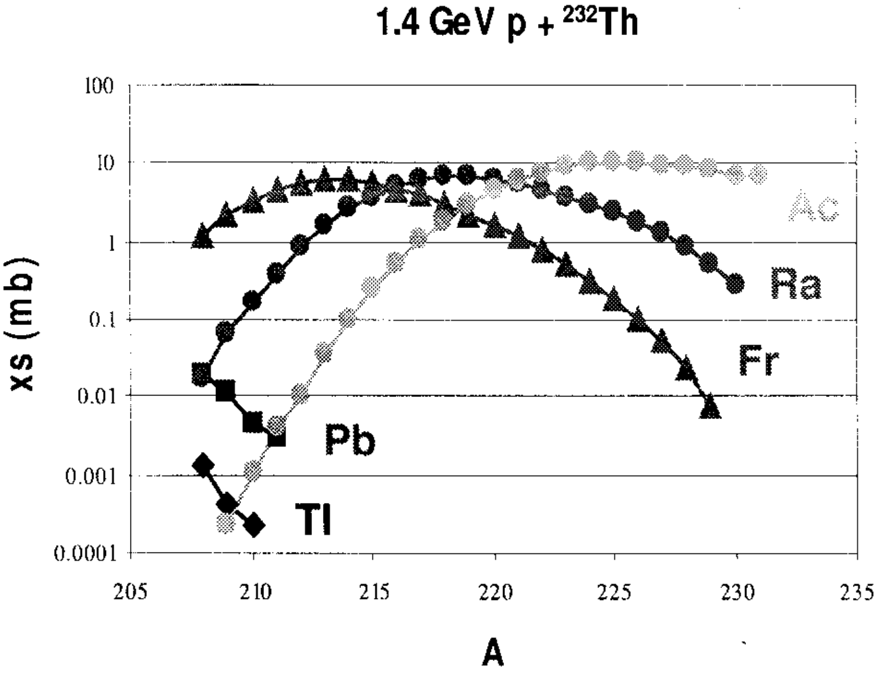

1.4 GeV p + ^{232}Th
100
10
1
0.1
0.01
0.001
0.0001
xs (mb)
205
210
215
220
225
230
235
A
Ac
Ra
Fr
Pb
Tl

Fig. 4

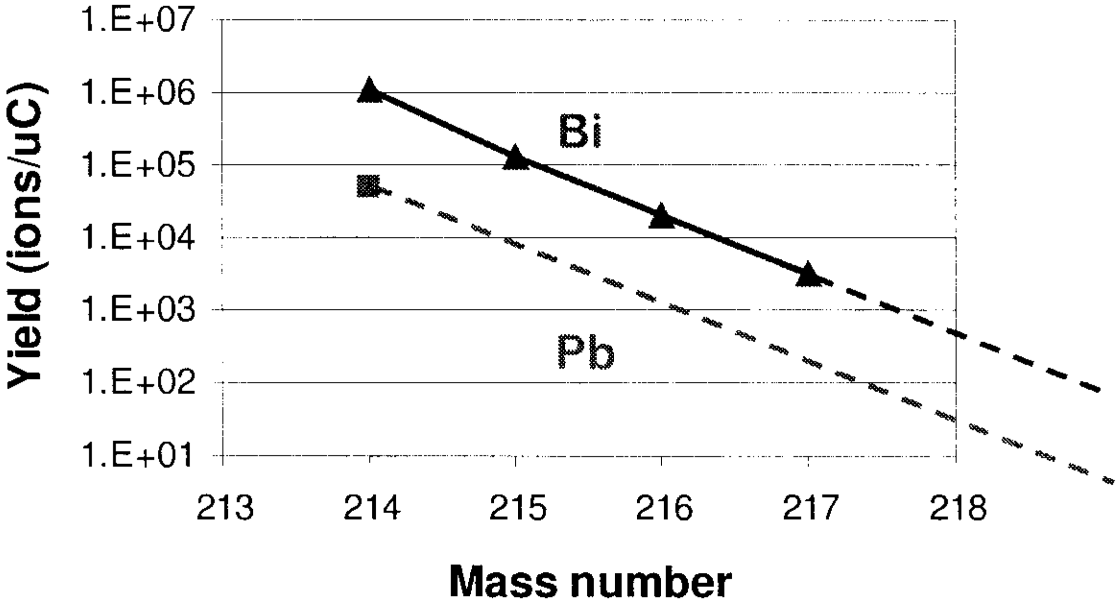

1.E+07
1.E+06
1.E+05
1.E+04
1.E+03
1.E+02
1.E+01
Yield (ions/uC)
213
214
215
216
217
218
Mass number
Bi
Pb